Atmospheric Research 183 (2017) 130–141

Contents lists available at ScienceDirect

Atmospheric Research

journal homepage: www.elsevier.com/locate/atmosres

Lightning jump as a nowcast predictor: Application to severe weather events in Catalonia

C. Farnell*, T. Rigo, N. Pineda

Meteorological Service of Catalonia, C/Berlin, Barcelona, 38-46, Spain

ARTICLE INFO

Article history:
Received 12 April 2016
Received in revised form 12 August 2016
Accepted 25 August 2016
Available online 30 August 2016

Keywords:
Lightning jump
Severe weather
Nowcasting
Total lightning
Catalonia

ABSTRACT

Several studies reported sudden increases in the total lightning flash rate (intra-cloud+cloud-to-ground) preceding the occurrence of severe weather (large hail, wind gusts associated to thunderstorms and/or tornadoes). Named "Lightning Jump", this pattern has demonstrated to be of operational applicability in the forecasting of severe weather phenomena. The present study introduces the application of a lightning jump algorithm, with an identification of cells based solely on total lightning data, revealing that there is no need of radar data to trigger severe weather warnings. The algorithm was validated by means of a dataset severe weather events occurred in Catalonia in the period 2009–2014. Results obtained revealed very promising.

1. Introduction

Lightning jumps (LJ), defined as sudden increases in the total lightning flash rate (Williams et al., 1999) , tend to precede severe weather occurrences on the ground (e.g. Darden et al., 2010; Fehr et al., 2005; Kane, 1991; Lang et al., 2000; Pineda et al., 2011; Tessendorf et al., 2007; Williams et al., 1999) The sudden increase in lightning activity is believed to be a response to the rapid intensification of the updraft that leads to an increasing number of ice particle collisions and thus greater charge separation and lightning (Carey and Rutledge, 1996; Deierling et al., 2008; Goodman et al., 2005; Steiger et al., 2007; Wiens et al., 2005; Williams, 2001) . The trends in the total lightning (intra-cloud+ cloud-to-ground; IC+CG) flash rate have shown a better performance (as compared to CG flash rates) as a tool for severe weather warning decision support (Schultz et al., 2011) .

Gatlin and Goodman (2010) and Schultz et al. (2011) demonstrated the operational applicability of the total lightning jump algorithm developed by Schultz et al. (2009). Schultz et al. (2011) has tested this algorithm to a set of 711 thunderstorms, in order to analyze the quality of the prediction of severe weather phenomena. The results obtained in that analysis revealed very promising, obtaining good values of the probability of detection (~79%) and false alarm (~22%) indices. Chronis et al. (2015) had modified the preliminary algorithm of Schultz et al. (2009), expanding the LJ to a longer time period of the life cycle of a thunderstorm. Chronis et al. (2015) examined over 2200 storms using automated tracking and real-time data feeds, with the main goal of comparing objective metrics of intensity, in order to determine if storms with lightning jumps lasted longer and contained larger radar derived intensity metrics like Maximum Expected Size of Hail (MESH). These works also pointed out that the total lightning jump is much more effective for severe weather nowcasting, compared to other predictors used for the same purpose like the IC:CG ratio (Pineda et al., 2011) or changes in the dominant CG polarity (Carey and Rutledge, 1998; Lang et al., 2004; Pineda et al., 2016; Soula et al., 2004; Wiens et al., 2005) patterns also linked to severe weather but highly variable and thus not effective

Severe weather is understood hereafter as the presence of at least on of these phenomena in a thunderstorm: hail of diameter equal or over 2 cm, wind gusts with speeds equal or larger than 25 m/s, and tornadoes. Regarding the hail size, 2 cm is the most common threshold used in many studies made around the World (Cao, 2008; Schuster et al., 2005; Tuovinen et al., 2009) . However, Allen and Tippett (2015) have explained the set of a larger threshold for the US (1 in., 2.5 cm) motivated by operational purposes, arguing that observers use inches instead of cm. Nonetheless, some American authors (e.g. Cintineo et al., 2012) still use the 0.75 in. (1.9 cm) threshold.

The lightning jump algorithm is intended to warn about severe weather, identifying rapid increases in total lightning flash rate preceding severe weather manifestations. The lead time between occurrence of lightning jump and severe weather phenomenon varies

* Corresponding author.
E-mail address: cfarnell@meteo.cat (F. C.).

http://dx.doi.org/10.1016/j.atmosres.2016.08.021
0169-8095/

depending of the different studies, but most of them agree that lightning jumps occur several minutes in advance of severe weather. Williams et al. (1999) registered differences between 5 and 20 min. Dimitrova et al. (2011) observed lightning jumps in three types of thunderstorms: multi-cellular, super-cellular, and multi-cell system evolving to super-cell thunderstorm. In each case a lightning jump was detected, but showing different lead times on respect the severe weather occurrence. In particular, these differences were 12, 20 and 24 min on respect the three cases presented before. Steiger et al. (2007) presented an analysis exclusively for super-cells, with lead times between lightning jumps and severe weather between 5 and 30 min. In the same way, Goodman et al. (2005) found an average lead time of 12 min, while Williams et al. (1999) established a value of 7 min, for hail events. Finally, Metzger and Nuss (2013) studied 34 cases of severe weather, but only in 18 of them that lightning jumps preceding the phenomena were found. In those cases with occurrence of both, observation and lightning jump, the time difference was of 14 min in average.

The main aim of this study is the evaluation of the utility of using trends in total lightning activity for diagnosing the potentiality of severe weather in a thunderstorm. An adaptation of the Schultz et al. (2009) algorithm was applied and tested in Catalonia. A key feature of the present work is that the algorithm attempts to predict severe weather without the use of any radar observable. This not means that weather radar is not useful for the identification of severe weather phenomena (in fact, it has been used here for the validation of events), but the present paper intends to show how the use of the algorithm may forecast a large number of cases using only electrical data. The manuscript is divided as follows: first is the presentation of the area of study. Then, the severe weather database used in this work and the remote sensing networks, joined with the methodology are introduced. This section includes the characteristics of the algorithm, the relationship between lightning jumps and the database, and the contingency tables and the verification indexes. Next, results are presented, and, finally, the conclusions and a brief discussion are developed.

2. The study area

Catalonia is a region of 32.000 km^2 placed at the Northeastern of the Iberian Peninsula (Fig. 1), surrounded by the Ebro Valley (west), the Pyrenees (north), and the Mediterranean Sea (east and south). The region has a wide diversity of geographic features, with four main orographic systems: the Pyrenees range, west-east oriented, delimits the northern extension of the region, and with heights moving near 3000 m ASL; the PrePyrenees, moving parallel more or less 40 km at the south of the first one and peaks between 1500 and 2000 m ASL; and the Coastal and Pre-Littoral ranges, running both parallel to the coast, from South-west to North-east, and with heights around 500 m and 1000 m, respectively. Furthermore, several flat landscapes are placed on between some of these ranges. This terrain variability, combined with the high sea surface temperature of the Mediterranean Sea, is one the factors that favours the relatively high occurrence of severe weather phenomena in the region.

Severe weather affects Catalonia in different ways. Hail mainly hit flat areas in western and the central Catalonia (Fig. 2), and are more important specially in Summer (Aran et al., 2007; Farnell and Llasat Botija, 2013; Rigo and Llasat, 2016; Rigo and Pineda, 2016) . Because of the severity of this phenomenon, the hailstorms produce important economical losses, mainly in the areas where agriculture plays an important role in the economy. During the period 2000–2009 the average economical loses were of 15 M € per year only in crops (Aran and Pena, 2009) . Tornadic and straight winds associated to thunderstorms events have a different geographical distribution. In the first case, tornadoes mostly occur in the coastal areas, and in some cases are waterspouts (Gayà et al., 2011) . Furthermore, some other case was registered in flat areas. Anyhow, tornadoes in Catalonia do not produce damages as important as hail, with the exception of those few cases that hit populated areas (Bech et al., 2007, 2011). Finally, strong wind gusts associated with thunderstorms are relatively common in the region, mainly in areas similar to the affected by hailstorms (Gayà et al., 2011; López, 2007; Ramis et al., 1997) , but the number of documented cases is relatively low, mainly because the damages produced are lower than the caused by hail and, moreover, the phenomenon is not as visually spectacular as tornadoes. A review of episodes with wind gusts exceeding 25 m/s as recorded by the Automatic Weather Stations network of the Meteorological Service of Catalonia resulted in a list of 65 events for the period 2007–2015. It is important to remark that observations had to be more or less coincident in time and space with lightning activity. This value is between the number of hail cases (maximum) and tornadoes (minimum), but the relevance in the press is clearly lower than the other two phenomena.

3. Data and methodology

3.1. Data

3.1.1. Database

Case study episodes was selected from the Severe Weather Database (hereafter SWDB) of the Meteorological Service of Catalonia (hereafter, SMC), which includes hail events, wind gusts associated to thunderstorms, and tornadoes in Catalonia from 2004 to 2015 (Rigo et al., 2015) . The wind speed threshold associated with gusts was reduced in relation to the original definition (25 m/s to 20 m/s, see the Introduction section). The cause is the observation of many reported events with strong damages in which the measured speed have not reached the original threshold in any automatic weather station. Although older severe weather reports exist, the SWDB was restricted to these twelve years because this period encompasses the same uniform and reliable remote sensing data quality. The process to identify, analyze, validate and finally include a severe weather event was the following. The information sources, similar to the used by other climatology works (e.g. Schuster et al., 2005; Tuovinen et al., 2009) , include technical reports, local or regional newspapers, local spotters, social networks and other internet sources, or information collected by the technical staff of the SMC. The description of each event considers the following information: date, time, coordinates type of phenomenon, and magnitude if it is possible.

In all the events, the same procedure was applied. The initial step was the identification of the characteristics associated with the phenomenon (date, time, coordinates, type of phenomenon, and its magnitude), if it is possible. Products used for validation, detailed later on, included: reflectivity radar animations, maps of lightning strokes, and wind, hail and rainfall measurements from automatic weather stations or hail-pads, if they are available. All the data comes from the SMC networks. All those cases that could not be validated, were discarded. The validated events finally included in the database were divided into two types: those with information for all the fields, and those lacking of some information, mainly the magnitude of the phenomena. In some of the cases, the validation was made using photographs or registers provided by official spotters of the SMC.

To conclude this point, it is important to notice that the current database considers each event as it is, allowing different observations very close in time and distance of the same (or other) phenomenon. The preliminary objective is to have a set or registers as wide as possible and, if it is necessary, to reduce the set picking up only the more representative values (mainly, the maximum daily or hourly values, or those associated with damaged structures).

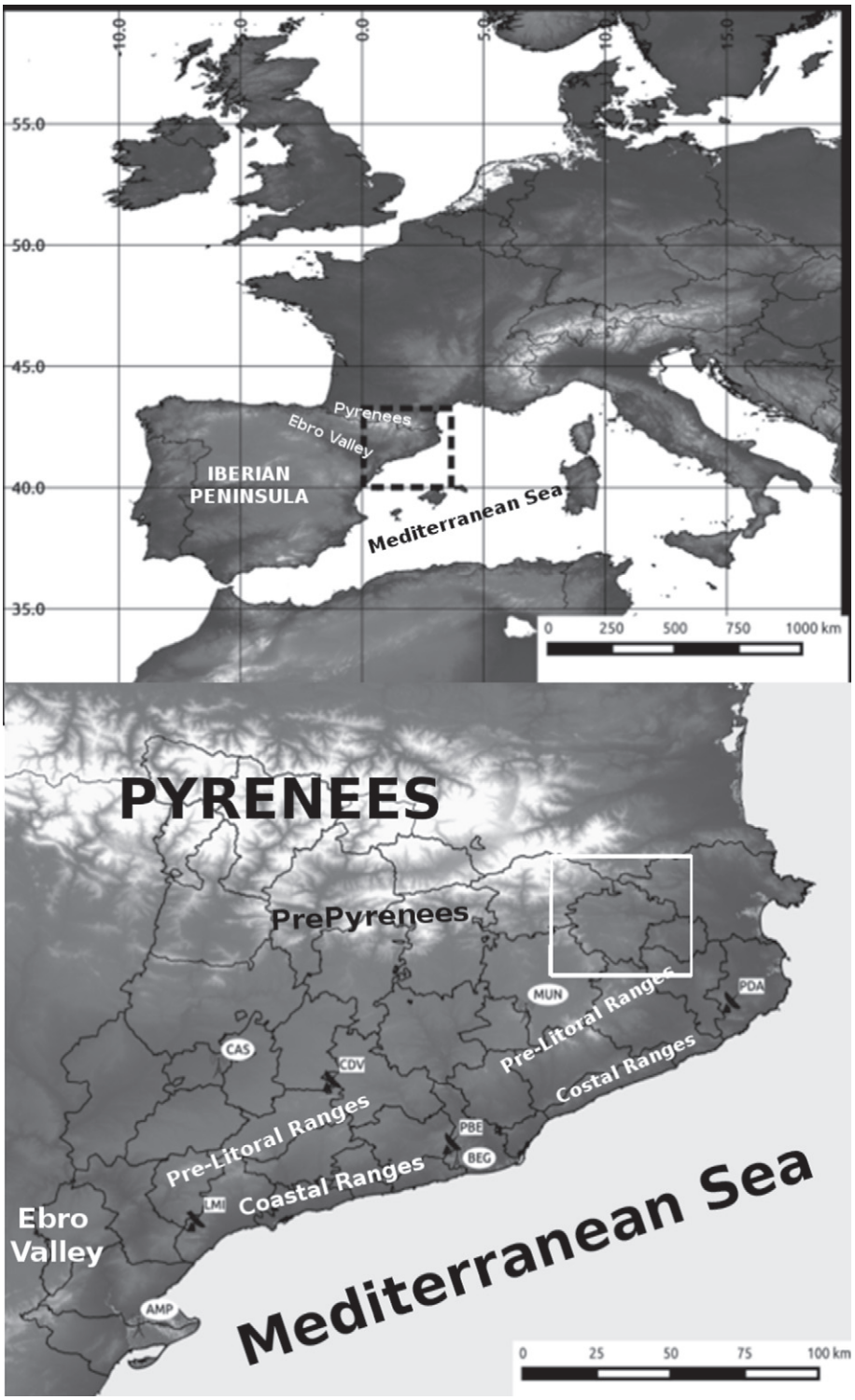

Fig. 1. Western Europe map, with the location of the region of study, including Catalonia in the NE of the Iberian Peninsula, marked by the square with black striped lines (above). Geographical topographical features of Catalonia, and the remote sensing networks (radar and lightning detectors) used in the study (below). The last figure included a white square corresponding to the zoom area presented in Fig. 9.

3.1.2. Lightning data

Lightning data comes from the lightning location system (LLS) operated by the SMC. It is composed by four VAISALA LS8000 stations covering Catalonia and its neighbours. The system detects and processes intra-cloud (IC) flashes and cloud-to-ground (CG) separately. The very high frequency (VHF) emissions generated by IC flashes are detected and processed by means of interferometry; the VHF sensor can locate a maximum of 100 detections per second with time resolution of 100-μs. The system computes azimuthal (two-dimensional) directions with the purpose of analyzing phase differences between antenna pairs of bursts pulse trains and provides locations and times of all located radio sources (Lojou and Cummins, 2006) . At least two sensors are necessary for generating the triangulation process. The detection range reaches ~250 km from the center of the network,

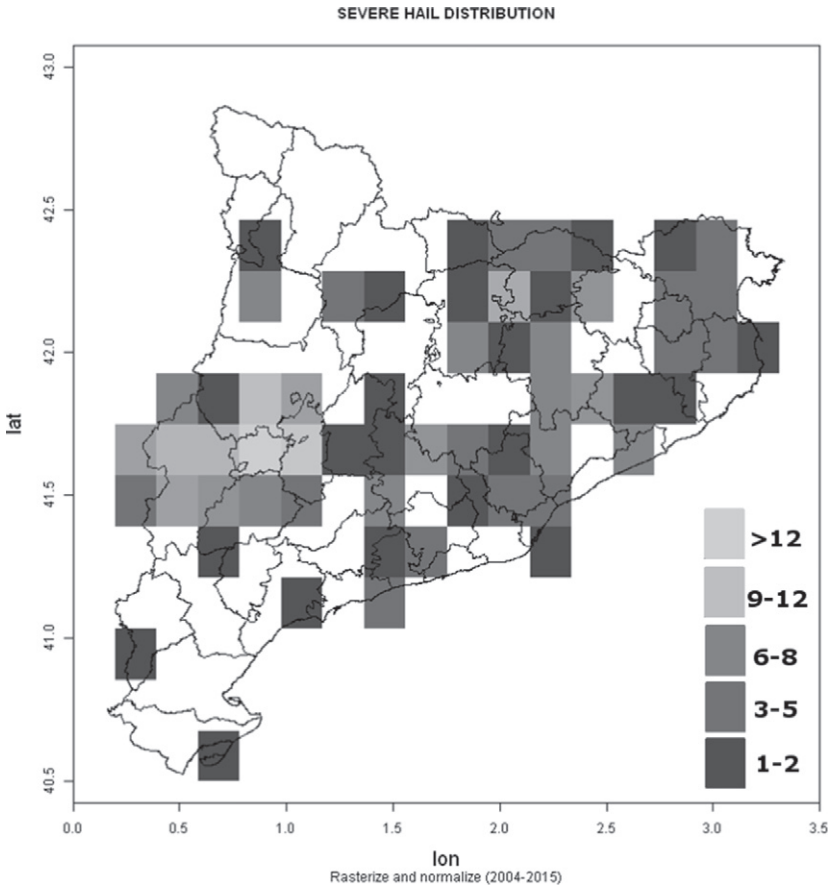

Fig. 2. Severe hail distribution for the period 2004–2015. The map was generated by means of pixels of 20 × 20 km^2, considering the maximum observation inside each pixel for each hail event.

covering Catalonia and the neighbour areas. The azimuthal precision of the sensors is 0.5deg RMS. The IC algorithm classifies, based on spatial and temporal criteria, each VHF source as part of an IC flash or, on the contrary, as a "singleton" (Williams et al., 1999) , this is, an isolated IC source. Singletons are not included in the IC flash counts, with the purpose of not overestimating the lightning flash rate.

The low frequency (LF) sensor of the LS8000 is able to detect the large current variations produced by CG return strokes. CGs are located by means of a combination of the Time-of-Arrival/Magnetic Direction Finding (TOA/MDF) techniques (Cummins and Murphy, 2009) . The detection efficiency inferred from experimental campaigns is 80–85% in the case CG flashes, while for IC detection efficiency is 70–75% (Montanyà et al., 2012; van der Velde and Montanyà, 2013).

3.1.3. Radar data

The radar network (XRAD) of the SMC is composed by four C-Band single polarization Doppler radars, which operate in two simultaneous modes:

(i) A long range (240 km) plan position indicator (PPI) product that is generated nearly instantaneously each 6 min, only with reflectivity fields.

(ii) A short range (130 km) and covers a great part of the troposphere over the radar, by means of 15 PPIs at different elevations (from 0.7deg until 30deg). In the second case, the fields provided are reflectivity and Doppler wind. More information about the XRAD can be found, for instance, in Rigo et al. (2010).

In the present work, even though radar data was not included in the complete procedure of the LJ algorithm, its utility was twofold, at the time of validation the results: In the first case, the generation of daily fields with reflectivity exceeding the 45 thresholds was used later (this is, not in real-time) in the validation process, and enabling to associate lightning jump position with the coordinates of a registered phenomenon. Moreover, the daily maps of the product POH45 (Probability of Hail using the TOP45 radar product) were used on those severe weather likely cases not recorded in the database, but it has seemed that evidences of severe weather is possible. The TOP45 is a radar product (Delobbe and Holleman, 2006) consisting in the detection of the highest elevation at which the 45 dBZ is exceeded, for each point of the radar coverage. This allows to have information of vertical development of rainfall cells using a 2D product. The POH45 (Aran et al., 2007) is generated combining the TOP45 and the isozero temperature level generated by a Numerical Weather Prediction Model (in our case, the WRF version 3.1.1, Shamarock et al., 2008, with 3 km resolution), by means of an empirically estimated equation. Maximum daily POH45 fields have only been used for the identification of hail events.

3.1.4. Surface observation data

Surface data used in this work came from three sources. Wind speed and direction is recorded by the network of 175 AWS of the SMC, a network designed to be representative of the complex topography of Catalonia. AWS data has a time resolution of 30 min.

Secondly, hail size was gathered with the network of hail-pads in the Western region of Catalonia (Rigo and Llasat, 2016) , which is managed by the Associació de Defensa Vegetal (ADV, Association for Plant Protection), while the data are processed by the University of Leon team. The network is composed of approximately 170 hail-pads,

with a more or less regular distribution of one hail-pad every 4 km^2 (Farnell et al., 2009; Fraile et al., 1992) . Although the covered area is not especially wide, the data provided by this network is very valuable, because this region is one of the most hit by hail in Europe (Punge and Kunz, 2016).

Finally, the network of spotters of the SMC (XOM) provides a list of observations of many weather phenomena. There are available data from this database since 2009. The distribution of the spotters enables the detection of many severe weather events that affect great part of Catalonia. Nonetheless, a high probability that in many cases the maximum values have not been registered exists. The network is composed by 233 spotters, divided in two categories (with some of them participating in both): those who provide weather information in a regular basis, and the ones who provide information about the watching of a severe weather (or any other adverse weather) phenomena to the forecast team of the SMC . In the present study, only those registers associated with severe weather were extracted from the database . The registers are considered as complete if they included a photography of the event, mainly in the case of tornado or hail.

3.2. Methodology

The Lightning Jump algorithm developed and tested in this study relies on the Schultz et al. (2009) one (hereafter, LJS09), which, at the same time, is similar to the Gatlin algorithm (Gatlin and Goodman, 2008) , but with some important differences (for instance, the LJS09 algorithm uses the standard deviation of 12 min of lightning data, instead of the weighted mean of 6 min of lightning data used by Gatlin). The original method consists in the identification of convective cells through radar tracking routines, like TITAN (Dixon and Wiener, 1993) or WDSS-II (Lakshmanan et al., 2007) , which uses a similar technique based on radar reflectivity exceeding a certain threshold. However, before going into details, an important difference must be highlighted. Contrary to the Schultz et al. (2009)algorithm, our method does not need radar information for cell identification and tracking. The thunderstorms are detected using exclusively total lightning data, with the following techniques: (i) Each 2 min, a query to the lightning database provides a file with the flashes detected during the previous 14 min. (ii) If any IC or CG flash is detected, the next steps are applied. (iii) A rasterization (this is, a conversion of points in a raster- or geo-referenced matrix) of the lightning flashes is made. A rasterization is applied, in order to transform lightning location points into a lightning density matrix with a spatial resolution of 1 × 1 km^2. The resulting raster will represent the number of lightning flashes located within each pixel. Afterwards, contiguous pixels with more than one flash are grouped into cells, by means of a neighbouring technique (see for instance, Rigo et al., 2010 or Dixon and Wiener, 1993).

Once a total lightning cell was detected, the analysis of the electrical activity is applied following Schultz et al. (2009) and Schultz et al. (2011): (1) for the "real time" (last 2 min), the mean rate of total of total lightning per minute is calculated; (2) if the value obtained in point (1) is equal or larger than 10, the other steps are activated and the steps (3) to (6) are applied. This threshold is defined to distinguish between severe and non-severe thunderstorms; (3) the same calculations as that of step (1) are done for the 12 previous minutes, grouped in 2 min intervals; (4) the results are subtracted for each consecutive interval, obtaining the time rate of change of the total flash rate (hereafter, DFRDT); (5) the standard deviation (σ) of the 5 DFRDT is calculated, defining the threshold of LJ as 2*σ. (6) The DFRDT for the last time period (real-time) is calculated. If this value exceeds the threshold defined in (5), the warning is activated.

Fig. 3 shows a comparison of the identification of a cell considering different radar techniques (for all the precipitating cell — straight lines, or for the convective regions — dotted lines), and the presented in this paper (grey shaded area). The figure also shows how isolated flashes (marked with an arrow) are not included in the region of interest. This is an example of how the current technique performs a better identification of the more active areas. For this reason, the splitting and merging processes are less probable to be produced into this concentrated cells. No cases were found for the whole set of analyzed events, which includes 515 tracked cells. However, the observation of these processes considering tracking with radar is possible. Some values can help to understand better the differences in magnitude of the different cells. From the 57,059 analyzed cells, the area values presented a maximum of 62 km^2, a median of 3, a mean of 5.1, and standard deviation of 5.5 km^2 (Table 1). Compared to other works dealing with the same region, the values obtained for the radar precipitating cells (reflectivity over 12 dBZ) in Rigo et al. (2010) were in average of 509 km^2. Furthermore, in the case of convective cells (those with reflectivity echoes exceeding 35 dBZ, mainly associated with hail but not necessarily) analyzed in Rigo and Llasat (2016), the 25, 50 and 75 percentiles values were 106, 194, and 438 km^2, respectively.

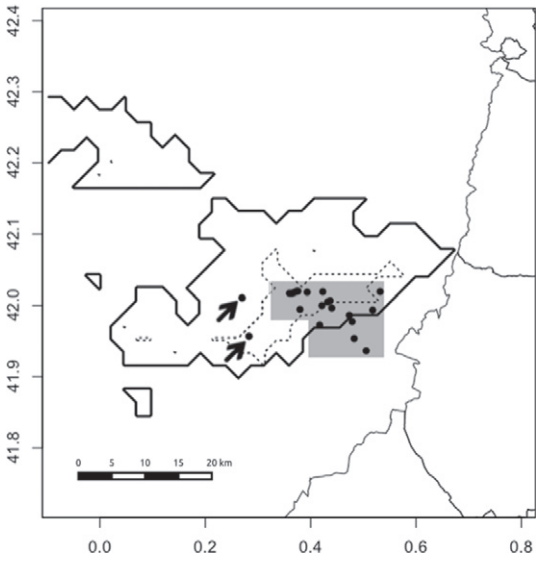

Fig. 3. Example of identification of cells for the case of the 4th of September 2014 (23:00 UTC): straight lines correspond to precipitating areas detected with radar (Z 12 dBZ), dotted lines show convective regions identified with radar, and, finally, grey shaded regions indicate areas with lightning activity (large black dots indicate flashes, both IC and CG types). Note that those pixels with a unique flash inside (marked with arrows) are rejected.

Fig. 4 shows an example of a tracking case occurred on 4th of September 2014 (23:00 UTC). Dots show the position of the centroid of the cell for each 1 min, considering darker colours as more recent cells (black colour corresponds to the cell position at 23:00 UTC). Lines correspond to the different size of the cell at three different times of the path (beginning, wide grey straight line; middle time, black narrow straight line; and end phase, black dotted line). This figure is an example of the common propagation of the cells, showing how the distance between correlative points in time never exceeds 3 km, and, moreover, they keep a rather constant area along the path.

Table 1
Comparison of the average area of cells tracked using only lightning data (present paper), radar at surface (Rigo et al., 2010), and volumetric radar data (Rigo and Llasat, 2016).

	Mean area (km^2)
Lightning data	5.1
Surface radar data	509
Volumetric radar data	194

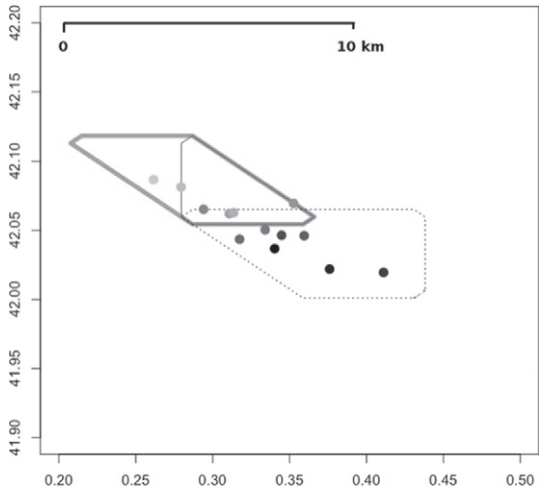

Fig. 4. Tracking of a TL (total lightning) cell identified for the same time that Fig. 3. Dots correspond with the position of the centroids along the 14 minutes tracked (as darker is the dot, much close to the "current" time is the centroid). Lines delimit the area of the cell: at the first time of the tracking (14 min before the current time, with wide straight line), in the middle time (7 min before the current time, with narrow straight line), and, at the current time (end part of the life cycle, with dotted line).

Although the algorithm is tracking cells, it cannot be considered as a classic tracking method (as, for instance, Dixon and Wiener, 1993 or Johnson et al., 1998). This is due to the fact that at a certain time, the procedure only seeks for the information from the last 14 min to the current time, but not in the previous stages of the cell, or in the future phases. It is important to keep in mind that the objective of the procedure is not known the previous or the future position of the cell, but not to detect sudden increases in total lightning activity. For this reason, it results difficult to compare it with other techniques. The fact that the tracking is made for 1 min time periods and for cells with a large number of total lightning flashes makes that practically all cells of interest (those associated with severe phenomena) are well followed across their path. Moreover, the algorithm focuses on the severe thunderstorms, for which the results of identification are very promising. On the other hand, it provides bad information for simple cells or even, multi-cells without a severe behaviour. Although the values are not completely conclusive, because of the reduced set of cells that verified the condition for applying the technique (only 515 cases), the distance between centroids per minute presents a maximum of 4 km, a mean value of 0.7, a median of 0.6, and standard deviation of 0.5 km, which are values similar or lower than the observed in the other studies cited for the same region.

3.3. Dataset

The present analysis relies on 48 daily episodes extracted from the SWDB. 43 of those days registered hail, while the other 5 were wind gust or tornado cases. The criteria of selection of the cases is based mainly in the amount of information available for each episode, which has dramatically increased in the last years because of the development of the social networks and the growing of the number of users of them (Table 2 and Fig. 5). The analysis of the data is made following the proposed methodology of the "Event day" (Brooks et al., 2003) , in which at least one phenomenon on a day at a specific position, being the mean expected value of the event equal to the probability of the event occurring, which value moves from 0 to 1.

The application of the LJ algorithm resulted in the activation of a LJ warning in 39 of the 48 episodes. Fig. 6 shows examples of different types of severe weather phenomena analyzed in the present work. In seek of simplicity, the diverse observations of severe weather reported in each event were reduced to a unique, representative observation (Fig. 7). Namely, the most important was selected, like in similar works (Cintineo et al., 2012; Schuster et al., 2005; Tuovinen et al., 2009) .

The last step of the work was the validation of the methodology, by means of the use of skill scores and a table of contingency (Haklander and Van Delden, 2003; Wilks, 2011) . The technique was applied to each event day, considering the main thunderstorms observed for each case.

Table 2
Set of selected events, including the date and the time, the magnitude (M), the type (Ty) of the phenomena (H — Hail; W — Waterspout; DB — Downburst), the number of LJ recorded (LJ), the values ¿0.8 of Probability of hail (Yes or No), the largest lead time (LT) between the LJ and Observations, and finally, the latitude (lat) and longitude (lon).

Date	Time	M	Ty	LJ	POH > 0.8	LT (min)	Lat	Lon
17/09/2007	15:00	5	H	3	NA	4	41.64	0.84
18/04/2008	15:00	3.5	H	2	NA	4	41.69	1.98
24/05/2008	18:15	1.5	H	0	NA	NA	41.79	0.50
11/09/2008	16:45	2	H	6	NA	−38	41.59	0.66
05/06/2009	17:30	3	H	5	NA	NA	42.25	0.97
25/06/2009	16:45	3	H	2	NA	90	41.73	1.51
26/06/2010	16:30	1	H	3	NA	21	41.52	0.88
04/07/2010	17:45	1.5	H	3	NA	25	41.69	0.86
02/08/2010	19:15	3	H	12	NA	28	41.75	0.88
12/08/2010	18:45	2	H	10	NA	74	41.19	1.46
31/08/2011	14:15	3	H	2	Y	−65	41.64	0.94
02/09/2011	17:00	1	H	3	Y	−37	41.60	0.41
03/09/2011	13:15	NA	H	11	Y	2	41.27	0.91
10/04/2012	21:25	NA	W	0	NA	NA	41.47	2.08
12/05/2012	13:00	1.5	H	0	Y	NA	41.42	2.03
13/05/2012	22:00	1	H	0	NA	NA	41.67	0.46
20/05/2012	16:15	4	H	4	Y	76	41.88	2.18
28/05/2012	10:30	1.5	H	0	NA	NA	41.88	2.62
03/06/2012	13:45	1	H	4	Y	−11	41.90	2.50
01/07/2012	14:30	1	H	2	Y	−6	41.93	2.26
05/07/2012	10:00	1	H	1	N	NA	41.47	2.24
27/07/2012	17:00	6	H	14	Y	55	41.63	0.90
05/08/2012	17:45	3	H	8	Y	NA	41.79	0.79
21/10/2012	18:30	NA	H	9	Y	47	41.74	0.59
27/10/2012	18:30	NA	H	0	NA	NA	41.93	2.26
18/06/2013	19:00	2.5	H	5	N	−9	41.67	0.46
10/07/2013	12:30	NA	W	1	Y	NA	41.08	1.20
14/07/2013	17:15	NA	W	0	NA	NA	41.3	2.17
19/07/2013	14:00	3.5	H	4	Y	26	41.66	0.98
23/07/2013	17:30	2.4	H	0	NA	NA	41.80	0.88
16/08/2013	16:00	3.5	H	7	Y	30	41.80	2.50
10/09/2013	21:00	NA	H	7	Y	NA	41.32	1.18
11/04/2014	14:30	4	H	0	NA	NA	42.05	3.10
17/06/2014	15:15	4.5	H	13	Y	13	42.18	2.49
02/07/2014	14:00	2	H	9	Y	36	42.07	1.83
20/07/2014	23:30	NA	W	6	Y	NA	41.26	2.13
04/09/2014	18:00	3	H	6	Y	NA	40.96	0.32
06/09/2014	18:00	1	H	7	N	71	41.79	1.29
09/09/2014	18:00	2.5	H	12	Y	33	41.47	1.53
14/09/2014	16:30	3	H	5	NA	2	41.56	0.57
15/09/2014	15:30	NA	H	6	Y	NA	42.05	3.1
16/04/2015	23:30	40	DB	11	Y	NA	41.72	0.59
09/06/2015	16:30	6	H	7	Y	39	42.05	2.27
23/06/2015	18:30	1.5	H	3	Y	59	41.40	2.17
18/07/2015	14:15	3	H	15	Y	55	41.64	0.93
24/07/2015	15:30	5	H	7	Y	120	42.05	3.11
31/08/2015	19:00	NA	H	2	Y	10	41.85	0.59
26/09/2015	16:45	4	H	3	Y	86	41.75	0.66

4. Results

In order to analyze the different warnings triggered during the selected episodes, the location of the severe weather observations

Fig. 5. Pictures showing damages or hail sizes of two different episodes shown in Table 1: 5th July 2012 (above) and 4th September 2014 (below).

and the position of the LJ warning are plotted for each case. Maximum reflectivity fields (with values exceeding 45 dBZ) are included to help the interpretation of each situation. Fig. 8 shows in the parts (a) and (b) of the panel the clear relationship between the position of the severe weather phenomena and the LJ warning location. Furthermore, the time of occurrence between diagnosis or forecast (since here, the LJ) and the observation is clearly related. This relationship is easily detected because the time of occurrence of each LJ and phenomenon is included in the plot. Using this methodology, it results easy to track the thunderstorms trajectory, and it can be observed how the LJ takes places first, followd by the severe weather phenomenon few minutes after. The use of the $Z \geq 45$ dBZ daily plot allows to identify more clearly the more severe part of each thunderstorm.

However, not all the cases show a clear relationship like the previous one. For instance, Fig. 8 (c) shows a LJ triggered without any related surface observation. If the maximum daily POH45 > 0.8 (80% of probability of hail, which is considered as indicator of hail in this analysis) is plotted under the observations, the connection between LJ location and areas with the highest values is clearly indicated. In case studies lacking of surface severe weather observations, the POH45 > 0.8 was used instead as a severe weather indicator. POH45 > 0.8 allows to identify hail events, but it is useless to detect nor wind neither tornado events. Therefore, some LJ flagged as false alarm using the POH45 > 0.8 threshold may correspond to severe cases but from the wind or tornado category. Anyway, the number of situations with this problematic is below the 1% of the total set. In any case, this technique allows compensating the shortcomings of the database, removing a large case of unrealistic false alarms.

On the contrary, Fig. 8 (d) presents a case in which severe weather has occurred but no LJ warnings were activated. In those cases, the lightning activity of the thunderstorms did not fulfill the criteria described before for the activation of the warning. Fig. 7 shows two examples of cases in which the warning was not triggered. The first case presents a discontinuity on the trajectory, that makes that the thunderstorm was not detected in any case more than 6 time steps (of 1 min) and then, the algorithm cannot be activated. In the other case, the anomaly of the total lightning time evolution made that the DFDRT was elevated in some previous moments of the life cycle, making that the $2^*\sigma$ threshold was relatively high, being difficult to exceed it during the period of highest electrical activity of the thunderstorm. Finally, Fig. 7 shows an example of case with LJ but not observation of severe weather. This represents the reduced number set of events.

The lightning jump technique is used as a severe weather forecast tool. For this reason, it results interesting to know how early it can provide a warning, compared to the time of occurrence of the phenomenon observation. The difference between LJ observation

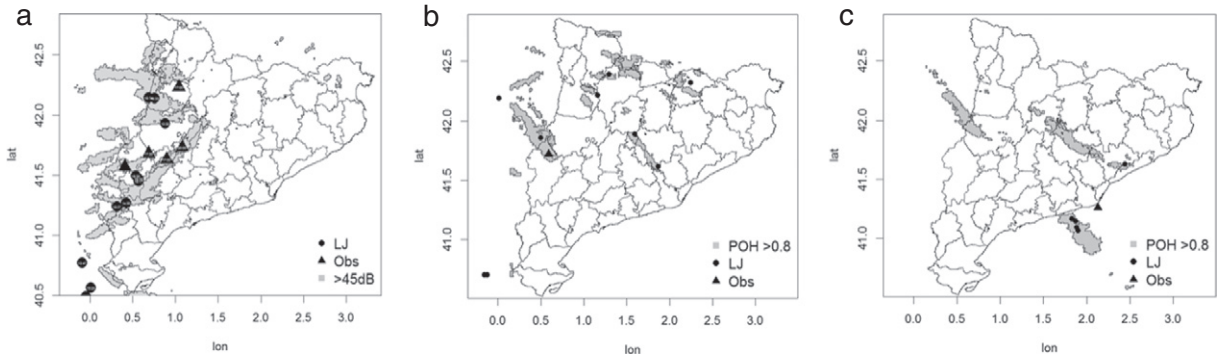

Fig. 6. Identification of lightning jumps (LJ) warning in different types of severe weather: (a) hailstorm; (b) waterspout; (c) downburst.

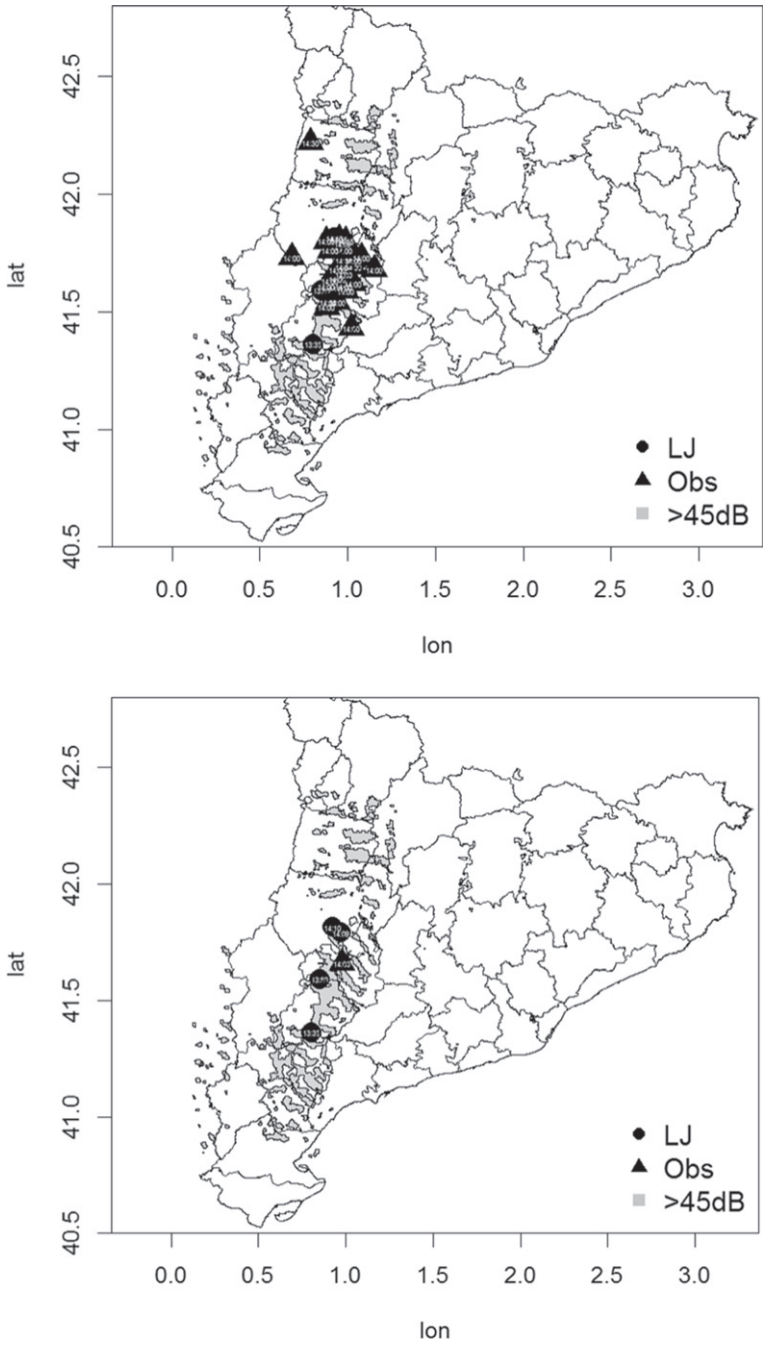

Fig. 7. Representative observations for a case of study 18th of June 2013. Above, all the observations registered in a event are shown. Below, the same event is presented showing only the most representative observations. Black dots show the LJ detections, triangles indicate the severe weather observations, and grey areas correspond to those pixels exceeding 45 dBZ reflectivity during the day.

and severe weather occurrence, known as lead time (LT), is calculated considering the time of occurrence of both events (LJ and observation at surface). In a case with multiple LJ triggerings, only the first one is considered. The time of the LJ is compared with the time of occurrence of the maximum value of severe weather. In most of the analyzed cases the lead time ranged from 15 to 45 min (Fig. 10), but is true that it exists many events in which TL occurred on time with the observation (this is, between 15 min prior the phenomenon and 5 min after this), but also another numerous group of events presented a lead time larger than 45 min. It is important to notice that the results in Fig. 10 are referred to all analyzed thunderstorms, meanwhile results shown in Table 2 indicates maximum LT for each event (in each event can occur many thunderstorms). Furthermore, a peak around 20 min before the occurrence of the severe weather is detected. Such a distribution of lead times is similar to Dimitrova et al. (2011) and other works like Williams et al. (1999). It must be taken into account that Fig. 10 presents not only those cases of LJ before the severe weather, if not also the events in which there are negative lead time. However, the last group (LJ after the severe weather occurrence) could be distorted, in the sense that in some situations severe weather reports are missing, because they have occurred in scarcely populated areas. Then, it is possible that results could be even better than the presented in Table 3.

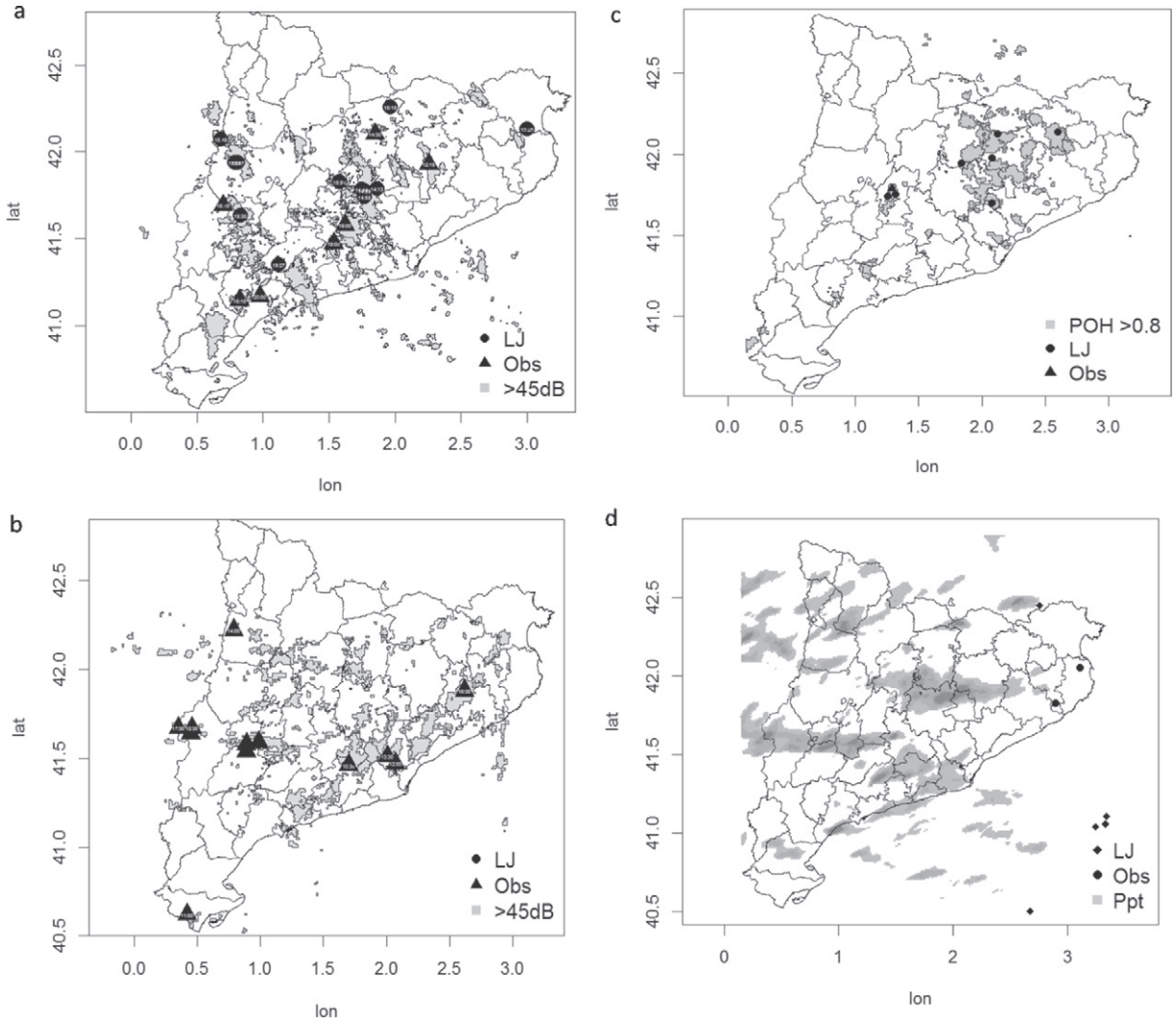

Fig. 8. (a) One case of daily representation of LJ warning, severe weather observations, and reflectivity over 45dBZ fields — 17th June 2014; (b) It shows severe weather observations and reflectivity over 45dBZ fields without LJ warning recorded — 20th May 2012 (Cont.) (c) and (d) represent the same case than the (a) but in the first case with maximum daily POH45 instead of reflectivity larger than 45dBZ — 09th September 2014 and the second case with daily precipitation instead of reflectivity larger than 45dBZ — 15th September 2014.

The usefulness of the LJ as a forecast predictor was validated through of the contingency table (see Table 3) and the skill scores (Haklander and Van Delden, 2003) . From the 48 studied events, 179 thunderstorms were selected. In 68 of them a LJ was registered and severe weather phenomena occurred (from the the database or the POH45 product); in 8 of the analyzed thunderstorms, LJ was triggered but there were no evidences of severe weather occurrences; other 40 thunderstorms produced severe weather phenomena, but LJ was not registered in their life cycle; finally, 63 of the analyzed convective cells not presented neither LJ or severe weather. It is important to have in mind that in the cases of thunderstorms that occurred over areas sparsely populated is possible that some severe weather phenomena went unnoticed. In any case, the set of cases are only below 5%(probably less) of the whole group of thunderstorms.

The verification indices showed very positive results, with an elevated rate of success. For instance, the Percent Correct (PC) registered a value of 0.73, this is, more than 70% of cases of severe weather were well forecast by the LJ algorithm. Furthermore, the number of false alarms, represented by FAR, presented a very low value (0.10). This means that only 10 of each 100 thunderstorms for which the algorithm forecast severe weather, had not observation. As it has said before, it is possible that this index was even lower. Other indices, such the Hit Rate (H) has also an elevated value (0.62), indicating a high number of cases with observations well forecast. The bias presents a value of 0.70, indicating that the number of events with severe weather was larger than the presented a LJ. In any case, the value is close enough to 1 and it can be considered positive results.

$$PC = \frac{(a+d)}{n} = 0.73$$
$$H = \frac{a}{a+c} = 0.62$$
$$FAR = \frac{b}{a+b} = 0.10$$
$$CSI = \frac{a}{a+b+c} = 0.58$$
$$B = \frac{a+b}{a+c} = 0.70$$

5. Discussion

An algorithm was developed to identify lightning jumps in the total lightning activity, to be used as forecast tool to warn about

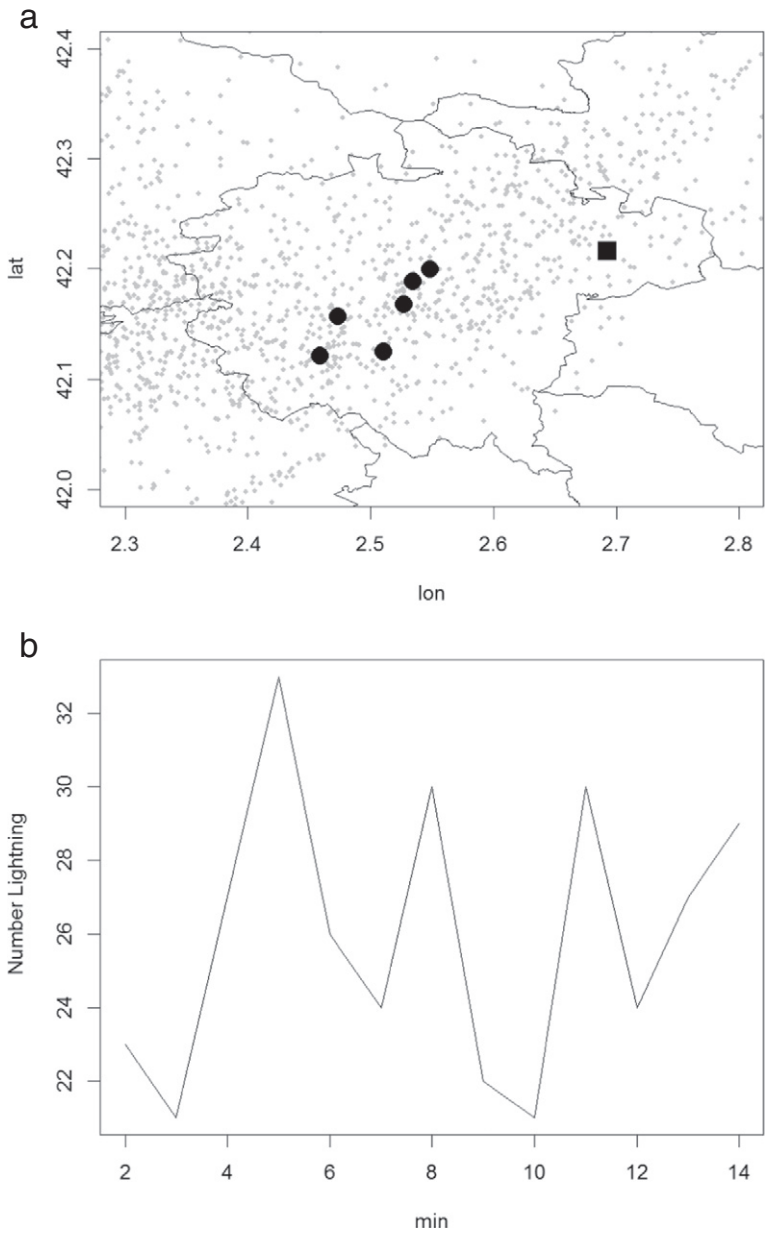

Fig. 9. (a) Centroids associated with the trajectory of the total lightning cells (black dots and square). The square is the last observation, which is not associated with the previous points (dots), because the distance criterion is not satisfied. Lightning flashes positions for the 14 min period were indicated with small grey dots. The area was marked with a rectangle in Fig. 1 (b) Total lightning evolution during a period of 14 min .

severe weather. The results presented in this study confirm that total lightning can be solely used (without any radar product) to warn about impending severe weather. This issue is important in the sense that countries with low budgets may forecast most of severe weather events occurring in their territory. The meteorological agencies only need spending some money on a lightning detectors network, instead of the high amounts of money necessary for the implementation of a weather radar network. Anyway, the proposed method has some advantages, but also inconveniences. The positive aspects of the use of lightning data for the identification of the cells are the following. Firstly, the LJ algorithm is only activated when lightning are observed and for those cells that can be considered as thunderstorms. This point is important, taken into account that in some images more than 30 radar cells can be identified but only few (or even none) of them have electrical activity. Moreover, the time line of radar images for the XRAD network is 6 min. This implies that the LJ algorithm only could be applied a third of the times that currently runs. In any case, one of the future lines of work is the development of a technique combining both identification algorithms, taking advantage of the positive points of each one, or, at least, the use of radar for validating the electrical cells identified in real-time. In any case, and how it was presented in the Data section, the radar data was used for validating the relationship between the detection of a lightning jump and the occurrence of a severe weather phenomenon. It should also be noted that the presented technique can be used as a complementary tool with, for instance, the nowcasting algorithm made with radar fields used in the SMC. In this sense, the radar procedure results more useful at the time of the tracking and nowcasting of the path for the whole precipitating clouds. On the contrary, the total lightning technique allows the identification of the most active cells. Those cells, or part of clusters, are more prone to be generators of severe weather phenomena

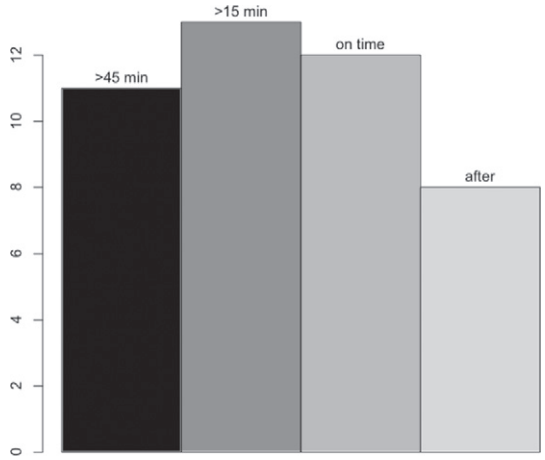

Fig. 10. Lead time distribution, considering different time intervals.

in the next 30 min. Then, the combination of both algorithms is a very powerful tool for surveillance tasks.

In any case, the use exclusively of lightning data produces a large number of severe weather cases in which the algorithm not produced any alarm. According to Table 2, the algorithm have a large number of miss events (more or less a 22%, which is less than the observed in Schultz et al., 2011). However, it existed a coincidence in most of the cases in which the algorithm didn't work: the thunderstorms not were associated with deep convection. This occurs in two type of situations: waterspout phenomena (probably they may be catalogued as F0 tornadoes in the United States), and hail events in mountainous areas. Moreover, in most of those episodes weather radar was also not capable of detecting any feature associated with severe weather, because of the characteristics of the thunderstorm that produced the severe weather.

Another benefit of the solely use of total lightning data, which is available in a real-time feed, is that the activation of the algorithm is not confined to the radar timeline. This means that the algorithm may be executed at user's convenience. Tracking algorithms needing radar data operating in a 5 to 10 min frequency may miss the LJ. The main inconvenience of the new technique, in relation with the original algorithm, is that the identification of any cell is less robust, in the sense that radar information is more continuous in space and in time (this is, a radar cell will maintain its shape for more time intervals than a lightning one, which is more morphing in time). Anyway, it must be noted that the main objective of the algorithm in not the tracking of thunderstorms, but the issuing of severe weather warnings. However, as it is presented in the description of the algorithm section, for severe thunderstorms (which are the real objective of the procedure), the identification results are better in this case, because of the continuity in time of the total lightning rates, and, moreover, of the tracking for shorter time periods (1 min in our case, instead of the 5 to 15 min in the case of radar). Besides this, the processes of merging or splitting of thunderstorms are more probable when lightning data are combined with radar fields. However, for the whole dataset of cases severe or near to severity thunderstorms, it was not found any situation of splitting or merging. This is due to the reduced size and more concreted to the more intense area of the thunderstorms selected in the present algorithm. The differences in size, 5 km^2 in average, for the cells in the present case, instead of the 195 km^2 for thunderstorms observed with radar or 509 km^2 in the case of lightning combined with radar, can explain this difference at the time of observe those processes. Finally, another point to consider is that the application does not use any threshold of total lightning flashes observed into the thunderstorm, differing the original (Schultz et al., 2009) , which proposed the detection of 10 flashes. The reason is the way how the cells are identified. In the original algorithm, cells, detected with the 20 dBZ radar reflectivity threshold, could contain more than one individual cells. However, in the new technique, the thunderstorms are clearly separated and, in any case, must verify some conditions on respect the number of flashes per pixel and the numbers of pixels. This makes that the procedure is centered exclusively in the electrical cells. In any case, it is possible that in the future, a threshold could be considered, in order of focusing only in those more active thunderstorms.

Table 3
Contingency table of the thunderstorms analyzed.

		Observed		
		Yes	No	
Forecast	Yes	68 (a)	8 (b)	76
	No	40 (c)	63 (d)	103
		108	71	179 (n)

6. Conclusions

Many authors have studied the relationship between the presence of lightning jumps (LJ) and the occurrence of severe weather phenomena associated with a thunderstorm. Most of them agree at the time to confirm the quality of LJ as a good forecaster tool. In the present work, a modification of the Schultz et al. (2009) algorithm was applied in Catalonia, testing its performance in 48 severe weather events, being most of the cases of hail. In 39 of them it has detected LJ.

The plotting of daily occurrences of LJ and severe weather observations helps to reinforce the understanding of the relationship between both stages: firstly, the sudden increase of the electrical activity in the thunderstorm, and, some kilometers further on, the occurrence of the severe weather. Moreover, when validating the algorithm, the combination of the unique information with daily fields of reflectivity that exceeds the 45 dBZ threshold allows to track the path of the thunderstorm. In those cases without severe weather observations, the use of the POH45 (Probability of Hail using the TOP45) product has confirmed, at least for hail cases, the occurrence of severe weather. This is a good new, in order to complete the database of severe weather in the region with remote sensing data.

The lead time between the detection of the LJ and the occurrence of the severe weather phenomenon is very variable. LJ were detected between 90 min before and 30 min after the severe weather observation. Moreover, not always results easy to calculate, because in some events severe weather occur in a brief time period and it results in difficulty to establish which ones are associated with the LJ. The information provided by a LJ is always favourable, because, even in the worst case (LJ after severe weather) it confirms the presence of the severe weather.

The verification indices indicate that the algorithm of LJ allows a good forecast of most of severe weather events. The percentage of success is close to 75%, while the false alarms are equal to 10%. This results encourages the testing of the operative product during the 2016 campaign, in which the algorithm works in real time.

Acknowledgments

The authors wish to thank the Associacio de Defensa Forestal (ADV-Pla de Lleida) and to the Grupo de Fisica de la Atmosfera, from the University of Leon, and the Research Area of the Servei Meteorologic de Catalunya (SMC) for the data provided.

References

Allen, J.T., Tippett, M.K., 2015. The characteristics of united states hail reports: 1955–2014. E-Journal of Severe Storms Meteorology 10 (3).

Aran, M., Pena, J., 2009. Atmospheric circulation patterns associated with hail events in lleida (Catalonia), preprints. 5th European Conference on Severe Storms, ECSS.

Aran, M., Sairouni, A., Bech, J., Toda, J., Rigo, T., Cunillera, J., Moré, J., 2007. Pilot project for intensive surveillance of hail events in Terres de Ponent (lleida). Atmos. Res. 83 (2), 315–335.

Bech, J., Pascual, R., Rigo, T., Pineda, N., López, J., Arús, J., Gayà, M., 2007. An observational study of the 7 September 2005 Barcelona tornado outbreak. Nat. Hazards Earth Syst. Sci. 7 (1), 129–139.

Bech, J., Pineda, N., Rigo, T., Aran, M., Amaro, J., Gayà, M., Arús, J., Montanyà, J., van der Velde, O., 2011. A Mediterranean nocturnal heavy rainfall and tornadic event. Part I: overview, damage survey and radar analysis. Atmos. Res. 100 (4), 621–637.

Brooks, H.E., Doswell, C.A., III, Kay, M.P., 2003. Climatological estimates of local daily tornado probability for the United States. Weather Forecast. 18 (4), 626–640.

Cao, Z., 2008. Severe hail frequency over Ontario, Canada: recent trend and variability. Geophys. Res. Lett. 35 (14).

Carey, L., Rutledge, S., 1996. A multiparameter radar case study of the microphysical and kinematic evolution of a lightning producing storm. Meteorog. Atmos. Phys. 59 (1-2), 33–64.

Carey, L.D., Rutledge, S.A., 1998. Electrical and multiparameter radar observations of a severe hailstorm. J. Geophys. Res.-Atmos. 103 (D12), 13979–14000.

Chronis, T., Carey, L.D., Schultz, C.J., Schultz, E.V., Calhoun, K.M., Goodman, S.J., 2015. Exploring lightning jump characteristics. Weather Forecast. 30 (1), 23–37.

Cintineo, J.L., Smith, T.M., Lakshmanan, V., Brooks, H.E., Ortega, K.L., 2012. An objective high-resolution hail climatology of the contiguous United States. Weather Forecast. 27 (5), 1235–1248.

Cummins, K.L., Murphy, M.J., 2009. An overview of lightning locating systems: history, techniques, and data uses, with an in-depth look at the US NLDN. IEEE Trans. Electromagn. Compat. 51 (3), 499–518.

Darden, C.B., Nadler, D.J., Carcione, B.C., Blakeslee, R.J., Stano, G.T., Buechler, D.E., 2010. Utilizing total lightning information to diagnose convective trends. Bull. Am. Meteorol. Soc. 91 (2), 167–175.

Deierling, W., Petersen, W.A., Latham, J., Ellis, S., Christian, H.J., 2008. The relationship between lightning activity and ice fluxes in thunderstorms. J. Geophys. Res.-Atmos. 113 (D15).

Delobbe, L., Holleman, I., 2006. Uncertainties in radar echo top heights used for hail detection. Meteorol. Appl. 13 (4), 361–374.

Dimitrova, T., Mitzeva, R., Betz, H.D., Zhelev, H., Diebel, S., 2011. Lightning behaviour during the lifetime of severe thunderstorms. 6th European Conference on Severe Storms.

Dixon, M., Wiener, G., 1993. Titan: thunderstorm identification, tracking, analysis, and nowcasting—a radar-based methodology. J. Atmos. Ocean. Technol. 10 (6), 785–797.

Farnell, C., Busto, M., Aran, M., Andres, A., Pineda, N., Torà, M., 2009. Study of the September 17th 2007 severe hailstorm in Pla d'Urgell. Part I: fieldwork and analysis of the hailpads. Tethys: Journal of Mediterranean Meteorology & Climatology 6, 69–81.

Farnell, C., Llasat Botija, M.d.C., 2013. Proposal of three thermodynamic variables to discriminate between storms associated with hail and storms with intense rainfall in Catalonia (Proposta de tres variables termodinàmiques per discriminar entre tempestes amb pedregades i tempestes amb pluges intenses). Tethys: Journal of Mediterranean Meteorology & Climatology 10, 25–34.

Fehr, T., Dotzek, N., Höller, H., 2005. Comparison of lightning activity and radar-retrieved microphysical properties in eulinox storms. Atmos. Res. 76 (1), 167–189.

Fraile, R., Castro, A., Sánchez, J., 1992. Analysis of hailstone size distributions from a hailpad network. Atmos. Res. 28 (3-4), 311–326.

Gatlin, P., Goodman, S., 2008. Severe weather precursors in the lightning activity of tennessee valley thunderstorms. Preprints, 3rd Conf. on Meteorological Applications of Lightning Data, New Orleans, LA, Amer. Meteor. Soc., CD-ROM. 8.

Gatlin, P.N., Goodman, S.J., 2010. A total lightning trending algorithm to identify severe thunderstorms. J. Atmos. Ocean. Technol. 27 (1), 3–22.

Gayà, M., Llasat Botija, M.d.C., Arús Dumenjó, J., 2011. Tornadoes and waterspouts in Catalonia (1950–2009). Nat. Hazards Earth Syst. Sci. 11, 1875–1883.

Goodman, S.J., Blakeslee, R., Christian, H., Koshak, W., Bailey, J., Hall, J., McCaul, E., Buechler, D., Darden, C., Burks, J., et al. 2005. The North Alabama lightning mapping array: recent severe storm observations and future prospects. Atmos. Res. 76 (1), 423–437.

Haklander, A.J., Van Delden, A., 2003. Thunderstorm predictors and their forecast skill for The Netherlands. Atmos. Res. 67, 273–299.

Johnson, J., MacKeen, P.L., Witt, A., Mitchell, E.D.W., Stumpf, G.J., Eilts, M.D., Thomas, K.W., 1998. The storm cell identification and tracking algorithm: an enhanced wsr-88d algorithm. Weather Forecast. 13 (2), 263–276.

Kane, R.J., 1991. Correlating lightning to severe local storms in the northeastern United States. Weather Forecast. 6 (1), 3–12.

Lakshmanan, V., Smith, T., Stumpf, G., Hondl, K., 2007. The warning decision support system-integrated information. Weather Forecast. 22 (3), 596–612.

Lang, T.J., Rutledge, S.A., Dye, J.E., Venticinque, M., Laroche, P., Defer, E., 2000. Anomalously low negative cloud-to-ground lightning flash rates in intense convective storms observed during STERAO-A. Mon. Weather Rev. 128 (1), 160–173.

Lang, T.J., Rutledge, S.A., Wiens, K.C., 2004. Origins of positive cloud-to-ground lightning flashes in the stratiform region of a mesoscale convective system. Geophys. Res. Lett. 31 (10).

Lojou, J.-Y., Cummins, K.L., 2006. Total lightning mapping using both vhf interferometry and time-of-arrival techniques. International Conference on Lightning Protection, Kanazawa, Japan. pp. 391–396.

López, J.M., 2007. A Mediterranean derecho: Catalonia (Spain), 17th August 2003. Atmos. Res. 83 (2), 272–283.

Metzger, E., Nuss, W.A., 2013. The relationship between total cloud lightning behavior and radar-derived thunderstorm structure. Weather Forecast. 28 (1), 237–253.

Montanyà, J., Van der Velde, O., March, V., Romero, D., Solà, G., Pineda, N., 2012. High-speed video of lightning and X-ray pulses during the 2009–2010 observation campaigns in northeastern Spain. Atmos. Res. 117, 91–98.

Pineda, N., Bech, J., Rigo, T., Montanyà, J., 2011. A Mediterranean nocturnal heavy rainfall and tornadic event. Part II: total lightning analysis. Atmos. Res. 100 (4), 638–648.

Pineda, N., Rigo, T., Montanà, J., Van der Velde, O., 2016. Charge structure analysis of a severe hailstorm with predominantly positive cloud-to-ground lightning. Atmos. Res. 178-179, 31–44.

Punge, H., Kunz, M., 2016. Hail observations and hailstorm characteristics in Europe: a review. Atmos. Res. 176, 159–184.

Ramis, C., Arús, J., López, J.M., Mestres, A.M., 1997. Two cases of severe weather in Catalonia (Spain): an observational study. Meteorol. Appl. 4 (03), 207–217.

Rigo, T., Aran, M., Bech, J., Farnell, C., Mateo, J., Pineda, N., Ripoll, R., Serra, A., 2015. Discriminating downburst-producing and hail-bearing thunderstorms using total lightning and weather radar observations. 8th European Conference on Severe Storms, ECSS.

Rigo, T., Llasat, M.C., 2016. Forecasting hailfall using parameters for convective cells identified by radar. Atmos. Res. 169, 366–376.

Rigo, T., Pineda, N., 2016. Inferring the severity of a multicell thunderstorm evolving to supercell, by means of radar and total lightning. E-Journal of Severe Storms Meteorology 11 (2).

Rigo, T., Pineda, N., Bech, J., 2010. Analysis of warm season thunderstorms using an object-oriented tracking method based on radar and total lightning data. Nat. Hazards Earth Syst. Sci. 10 (9), 1881–1893.

Schultz, C.J., Petersen, W.A., Carey, L.D., 2009. Preliminary development and evaluation of lightning jump algorithms for the real-time detection of severe weather. J. Appl. Meteorol. Climatol. 48 (12), 2543–2563.

Schultz, C.J., Petersen, W.A., Carey, L.D., 2011. Lightning and severe weather: a comparison between total and cloud-to-ground lightning trends. Weather Forecast. 26 (5), 744–755.

Schuster, S.S., Blong, R.J., Speer, M.S., 2005. A hail climatology of the greater Sydney area and New South Wales, Australia. Int. J. Climatol. 25 (12), 1633–1650.

Shamarock, W., Klemp, J., Dudhia, J., Gill, D., Barker, D., Duda, M., Huang, X., Wang, W., Powers, J., 2008. A description of the advanced research WRF version 3: Ncar technical note tn-475+ str. . National Center for Atmospheric Research Boulder, Colorado, USA.

Soula, S., Seity, Y., Feral, L., Sauvageot, H., 2004. Cloud-to-ground lightning activity in hail-bearing storms. J. Geophys. Res.-Atmos. 109 (D2).

Steiger, S.M., Orville, R.E., Carey, L.D., 2007. Total lightning signatures of thunderstorm intensity over North Texas. Part II: mesoscale convective systems. Mon. Weather Rev. 135 (10), 3303–3324.

Tessendorf, S.A., Rutledge, S.A., Wiens, K.C., 2007. Radar and lightning observations of normal and inverted polarity multicellular storms from steps. Mon. Weather Rev. 135 (11), 3682–3706.

Tuovinen, J.-P., Punkka, A.-J., Rauhala, J., Hohti, H., Schultz, D.M., 2009. Climatology of severe hail in Finland: 1930–2006. Mon. Weather Rev. 137 (7), 2238–2249.

van der Velde, O.A., Montanyà, J., 2013. Asymmetries in bidirectional leader development of lightning flashes. J. Geophys. Res.-Atmos. 118 (24).

Wiens, K.C., Rutledge, S.A., Tessendorf, S.A., 2005. The 29 June 2000 supercell observed during steps. Part II: lightning and charge structure. J. Atmos. Sci. 62 (12), 4151–4177.

Wilks, D.S., 2011. Statistical methods in the atmospheric sciences. 100. Academic Press.

Williams, E., Boldi, B., Matlin, A., Weber, M., Hodanish, S., Sharp, D., Goodman, S., Raghavan, R., Buechler, D., 1999. The behavior of total lightning activity in severe Florida thunderstorms. Atmos. Res. 51 (3), 245–265.

Williams, E.R., 2001. The electrification of severe storms. Severe Convective Storms. Springer., pp. 527–561.